JOURNAL OF VIROLOGY, Nov. 1997, p. 8279–8288 Vol. 71, No. 11
0022-538X/97/$04.00+0

Mutational Analysis of the Role of Glycoprotein I in Varicella-Zoster Virus Replication and Its Effects on Glycoprotein E Conformation and Trafficking

SUZANNE MALLORY, MARVIN SOMMER, AND ANN M. ARVIN*

Department of Pediatrics and Microbiology/Immunology, Stanford University School of Medicine, Stanford, California 94305

Received 9 June 1997/Accepted 15 July 1997

The contributions of the glycoproteins gI (ORF67) and gE (ORF68) to varicella-zoster virus (VZV) replication were investigated in deletion mutants made by using cosmids with VZV DNA derived from the Oka strain. Deletion of both gI and gE prevented virus replication. Complete deletion of gI or deletions of 60% of the N terminus or 40% of the C terminus of gI resulted in a small plaque phenotype as well as reduced yields of infectious virus. Melanoma cells infected with gI deletion mutants formed abnormal polykaryocytes with a disrupted organization of nuclei. In the absence of intact gI, gE became localized in patches on the cell membrane, as demonstrated by confocal microscopy. A truncated N-terminal form of gI was transported to the cell surface, but its expression did not restore plaque morphology or infectivity. The fusogenic function of gH did not compensate for gI deletion or the associated disruption of the gE-gI complex. These experiments demonstrated that gI was dispensable for VZV replication in vitro, whereas gE appeared to be required. Although VZV gI was dispensable, its deletion or mutation resulted in a significant decrease in infectious virus yields, disrupted syncytium formation, and altered the conformation and distribution of gE in infected cells. Normal cell-to-cell spread and replication kinetics were restored when gI was expressed from a nonnative locus in the VZV genome. The expression of intact gI, the ORF67 gene product, is required for efficient membrane fusion during VZV replication.

Varicella-zoster virus (VZV) is the causative agent of chicken pox (varicella) and herpes zoster (shingles) (2). VZV is the smallest human herpesvirus, with a genome of approximately 125 kb, containing at least 69 distinct open reading frames (ORFs). It is related to herpes simplex virus types 1 and 2 (HSV-1 and -2), simian varicella virus, pseudorabies virus (PRV), and the other alphaherpesviruses (11). While these other viruses have at least four genes encoding glycoproteins within the short unique (U_S) region, including gD, gE, gG, and gI, VZV has only two, ORF67 and ORF68, which encode gI and gE, respectively. In HSV, which is the human herpesvirus related most closely to VZV, gD is required for penetration and direct cell-to-cell spread (35, 48). In the absence of a gD equivalent, VZV gE and gI may have essential functions in viral infection that are not characteristic of their counterparts in the other alphaherpesviruses.

Investigations of gE (gp I) and gI (gp IV) produced in cells infected with VZV, or from plasmid, vaccinia, or baculovirus vectors, demonstrate that these two glycoproteins form a noncovalently linked complex after their synthesis in the endoplasmic reticulum (ER) and that the complex is expressed on the cell surface (55). A site of interaction between gE and gI has been mapped to the N terminus of gI (34). The mature forms of gE and gI contain N- and O-linked glycosylation and are phosphorylated in mammalian and insect cells (26, 46, 54, 56).

Although ORFs of the gE and gI homologs have similar genome locations within the U_S region, there are significant differences between the products of these genes among the alphaherpesviruses. In VZV, gE is the most abundant glycoprotein, whereas it is a minor component of the HSV envelope (43). VZV and HSV gI have only 24% identity in amino acid sequence, and the sequence identity for the gE homologs is 27% (36). The gE gene products of VZV and HSV bind the Fc fragment of human immunoglobulin, but HSV gE has a stronger Fc receptor affinity (9, 12, 20, 31, 36, 40). The characteristics of gE and gI are not uniform in the alphaherpesviruses subfamily. For example, neither gE nor gE-gI complexes have Fc receptor function in PRV or bovine herpesvirus (BHV) (53, 58).

Infectious virus can be recovered after the deletion of gI or gE from HSV, PRV, BHV, and equine herpesvirus 1 (7, 23, 32, 37, 38, 52, 53). Nevertheless, these glycoproteins contribute to viral entry, cell-to-cell spread, and viral egress in vitro as well as to virulence and neurotropism in animal models (6, 7, 8, 15, 17, 18, 22, 28, 44). The functions of VZV gE and gI in viral pathogenesis in vivo have not been defined, but both glycoproteins are immunogenic in the human host and in the guinea pig model of VZV infection (4, 5, 24, 29, 30, 50).

Our objective was to investigate the functions of gI and gE in VZV by mutational analysis of ORF67 and ORF68, using a cosmid system (33). Since VZV replicates as a completely cell-associated virus in tissue culture, pure populations of mutant viruses cannot be obtained by homologous recombination. This obstacle to generating mutant virus strains has been addressed by ligating overlapping fragments, which represent the full-length genome of VZV into cosmid vectors (10). As was observed with PRV, cotransfection of the overlapping fragments results in recombination and the synthesis of infectious virus progeny (51). In our experiments, ORF67 and ORF68 were subcloned into plasmid vectors from the cosmid containing the U_S region of the genome, gene sequences were altered and ligated back into the cosmid, and the modified cosmid was cotransfected into permissive cells along with the three intact cosmids. This approach permitted an investigation of the ef-

* Corresponding author. Phone: (415) 723-5682. Fax: (415) 725-8040.

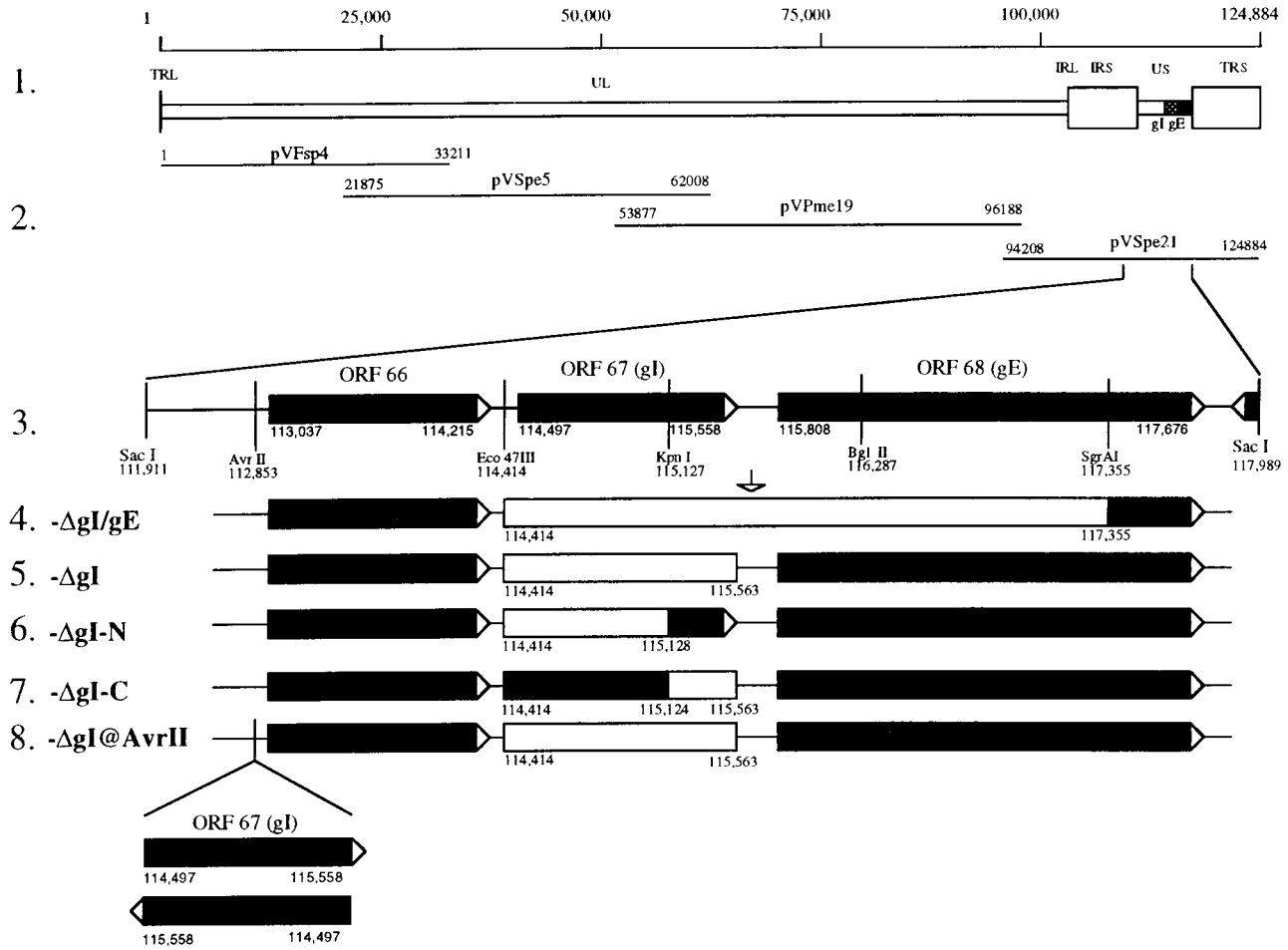

FIG. 1. Construction of cosmid vectors with deletions of VZV ORF67 (gI) and ORF (gE). Line 1 shows a schematic diagram of the VZV genome with the locations of the genes that encode gI and gE in the U_S region. Line 2 depicts the overlapping segments of the VZV genome used to construct the VZV cosmids. Line 3 shows the subcloned *Sac*I fragment that includes ORF67 and ORF68 (black boxes) with the restriction sites used to construct the deletions in ORF67 and ORF68 and the *Avr*II and *Sgr*AI sites used to insert the mutated fragments back into the cosmid. Lines 4 to 7 depict the deleted regions (open boxes) resulting in cosmids pVSpe21EID (ΔI/gE), pVSpe21ΔgI, pVSpe21ΔgI-N, and pVSpe21ΔgI-C, respectively. To restore gI, ORF67 was ligated into a unique *Avr*II site of pVSpe21ΔgI in each orientation, resulting in pVSpe21gI@Avr#14 (left-to-right orientation) and pVSpe21gI@Avr#9 (right-to-left orientation) (line 8).

fects of mutations made in the gI and gE coding sequences on VZV replication.

MATERIALS AND METHODS

VZV cosmids. Four overlapping fragments of genomic DNA from the Oka strain of VZV were ligated into SuperCos 1 cosmid vectors (Stratagene, La Jolla, Calif.); these cosmids were kindly provided by George Kemble, Aviron, Inc., Mountain View, Calif. (33). The genes for gI (ORF67) and gE (ORF68) are in the U_S region of VZV DNA which is in the cosmid pVSpe21ΔAvrII; the deletion of an *Avr*II site from the original cosmid vector at SuperCos 1 nucleotide 3359 produced a unique *Avr*II site at VZV nucleotide 112853 (Fig. 1). ORF67 extends from nucleotides 114497 to 115558, and ORF68 is located between nucleotides 115808 and 117676 (13) (Fig. 1, line 3). A mutant construct of the pVSpe21ΔAvrII cosmid, designated pVSpe21EID, was made to remove both ORF67 and ORF68 (Fig. 1, line 4). The pVSpe21ΔAvrII cosmid was digested with *Sac*I, generating a 6-kb fragment from nucleotides 111911 to 117989 that contained the gI and gE ORFs; this fragment was subcloned into a pBluescript KS$^-$ vector (Stratagene) to make plasmid pSac6A. pSac6A was digested with *Eco*47III at nucleotide 114414 and *Sgr*AI at nucleotide 117355. A 6.1-kb fragment was isolated, the *Sgr*AI site was reconstituted by linker insertion, and the remaining vector, with a deletion of gI and gE, was religated to form pSac8ΔSgr. pSac8ΔSgr was digested at unique restriction sites, *Avr*II and *Sgr*AI, resulting in a 1.5-kb fragment from which all of ORF67 and ORF68, except for 321 nucleotides at the 3′ end of ORF68, had been deleted; this fragment was ligated into the 33-kb fragment of pVSpe21ΔAvrII generated by *Avr*II and *Sgr*AI cleavage at nucleotides 112853 and 117355, respectively.

A second cosmid, pVSpe21ΔgI, was constructed to remove the complete gI coding sequence while leaving the ORF68 encoding gE intact (Fig. 1, line 5). An *Eco*47III site was introduced between ORF67 and ORF68 by the PCR method. Primers were designed beginning at VZV nucleotide 115558, using the primer sequence of GTTAAATAGCGCTAATTATCC, with base pair substitutions made to introduce an *Eco*47III site (underlined), or at the *Bgl*II site located at nucleotide 116287, using the primer sequence TTGGATTAAGATCTCCT TTAA. pSac6A was linearized with *Pst*I for PCR, and the ends of the resulting 729-bp fragment were digested with *Eco*47III and *Bgl*II. pSac6A was then digested with *Eco*47III and *Bgl*II, and the 7.2-kb fragment was ligated to the 729-bp PCR product. The resulting vector, pSac5ΔgIEco47III, was digested with *Avr*II and *Sgr*AI and ligated back into pVSpe21ΔAvrII, as described above, resulting in a variant of the pVSpe21 cosmid from which only the gI gene was deleted.

A third cosmid, pVSpe21ΔgI-N, was constructed to delete the N terminus of gI (Fig. 1, line 6). pSac6A was digested at the *Eco*47III (VZV nucleotide 114414) and *Sgr*AI (VZV nucleotide 117355) restriction sites, yielding a 6.1-kb band from which ORF67 and ORF68 were deleted. A separate digest of pSac6A with *Kpn*I (VZV nucleotide 115127) and *Sgr*AI resulted in a 2.2-kb fragment that contains and therefore repairs the loss of ORF68 and of the C terminus of ORF67 when ligated to the 6.1-kb fragment. The resulting plasmid, pSac12ΔgI-N, was digested with *Avr*II and *Sgr*AI to generate a 3.8-kb fragment which contained the gI sequence from nucleotides 115128 to 115558 only, with deletion of nucleotides encoding the N-terminal two-thirds of gI; this fragment was ligated into pVSpe21ΔAvrII, resulting in the cosmid pVSpe21ΔgI-N. The fourth cosmid, pVSpe21ΔgI-C, was constructed to delete the C-terminal residues of gI (Fig. 1, line 7). A 2.3-kb fragment was generated by digesting pSac6A with *Kpn*I; DNA was blunted with Klenow enzyme and digested with *Avr*II. The 2.3-kb fragment

was ligated into a 6.3-kb fragment derived from pSac5ΔgIEco47III, described above, that had been digested first with AvrII and Eco47III. The new vector, pSac5ΔgI-C, was digested with *Avr*II and *Sgr*AI and ligated into pVSpe21ΔAvrII.

Two cosmids, pVSpe21gI@Avr#9 and pVSpe21gI@Avr#14, were made in order to restore the deletion of the gI coding region from pVSpe21ΔgI (Fig. 1, line 8). The ORF67 sequence was generated by PCR using primers that were designed to introduce *Avr*II sites at each end of the 1.4-kb PCR product (underlined in the primer sequences below); the primer sequences were AAAATTCCCTAGGCCTGTTA and TCACAACGCCTAGGCAAAAC, starting at VZV nucleotides 114217 and 115632, respectively. pVSpe21ΔgI was then digested at its unique *Avr*II site, and the linearized cosmid and 1.4-kb PCR product were ligated to produce pVSpe21gI@Avr#9 and pVSpe21gI@Avr#14, which have the gI gene introduced in opposite orientations.

Before use in cotransfections, the intact and mutated pVSpe21 cosmids, and the other three VZV cosmids spanning the complete VZV genome, designated pVFsp4, pVSpe5, and pVPme19 (Fig. 1), were electroporated into Top 10F′ competent cells (Invitrogen Inc., Carlsbad, Calif.), grown in LB containing kanamycin and ampicillin, and purified by using a Qiagen plasmid maxiprep kit as specified by the manufacturer (Qiagen, Inc., Chatsworth, Calif.).

Transfection, virus isolation, and confirmation of mutations. Cosmids were digested with *Asc*I and mixed in water to final concentrations of 100 ng/μl for pVFsp4, pVSpe5, pVPme19 and 50 ng/μl for pVSpe21. Transfections were done with human melanoma cells, using 20 or 30 μl of the cosmid mix in 31.5 μl of 2 M $CaCl_2$ in water and HEPES-buffered saline. After transfection, the melanoma cells were kept at 37°C for 3 to 4 days, trypsinized, and transferred to a 75-cm^2 flask; plaques appeared 5 to 6 days after transfection with intact cosmids. Cells transfected with mutant cosmids were passaged at a 1:3 ratio every 3 to 4 days. Infectious virus recovered from transfections was propagated by inoculation of melanoma cells with virus-infected cells (27).

PCR was used to confirm the expected changes in fragment sizes in cosmids and recombinant virus DNA and to sequence the regions spanning the ORF67 (gI) deletions and ORF67 insertions into the *Avr*II site. VZV cosmid DNA was purified by using Qiagen columns, and recombinant virus DNA was recovered from infected cells by using DNazol (Gibco BRL, Inc., Grand Island, N.Y.). PCR was performed with Elongase enzyme mix (Gibco BRL). The primers used to assess deletions across ORF67 were TTTGCGTTTGCGTGTATGGA and TATGCGGTGTAGTTATCTGC, located at VZV nucleotides 113354 and 117112, respectively. The primers used to determine the sizes of insertions into the unique *Avr*II site were TTACCACCGCTTCCATCA and CCACACA AACATCACCTG, located at VZV nucleotides 112580 and 113686, respectively.

For Southern blot analysis, VZV genomic or cosmid DNA was cut with *Kpn*I, and the fragments were separated in a 0.7% agarose gel and transferred to a Hybond nylon membrane (Amersham, Inc., Arlington Heights, Ill.). A 1.6-kb fragment, resulting from an *Sgr*AI-*Hpa*I digest, which hybridizes to VZV DNA sequences 115670 to 117355, was used as a probe. The probe was labeled with digoxigenin, and hybridization was detected by using a chemiluminescent alkaline phosphate substrate (Genius luminescent detection kit) as instructed by the manufacturer (Boehringer Mannheim, Inc., Indianapolis, Ind.).

Infectious focus assay. Virus titrations were done by using infected melanoma cells serially diluted 10-fold in minimal essential medium with 10% fetal calf serum and added to 24-well dishes in triplicate (42). After incubation for 5 to 6 days, the wells were stained with crystal violet and plaques were counted. The average number of plaques in triplicate wells was divided by the number of cells in the inoculum to determine infectious foci per cell. Thirty plaques in each monolayer were measured, and statistical differences in plaque size were determined by Student's *t* test.

Western blotting. Aliquots of cell lysates from melanoma cells infected with VZV recombinants were boiled in sample buffer containing sodium dodecyl sulfate and 2-mercaptoethanol. The proteins were separated in a 10% polyacrylamide gel and transferred to a nitrocellulose membrane. After blocking with 5% nonfat milk in phosphate-buffered saline (PBS), the nitrocellulose membrane was incubated for 1 h at room temperature with a 1:50 dilution of a polyclonal antiserum against gE generated by injection of rabbits with a vaccinia virus recombinant expressing gE (anti-Vac-gE), kindly provided by Paul Kinchington, University of Pittsburgh, Pittsburgh, Pa. A biotinylated goat anti-rabbit antibody labeled with horseradish peroxidase was used to detect specific antibody binding to gE. A monoclonal antibody to gE, designated B5, was used, as well as the anti-gE monoclonal antibody 3B3, kindly provided by Charles Grose, University of Iowa College of Medicine, Iowa City.

Confocal microscopy. Melanoma cell monolayers in chamber slides (Lab-Tek, Inc., Naperville, Ill.) were inoculated with VZV-infected cells at a dilution of 1:8 (21). After 32 or 56 h, the cells were labeled with BODIPY TR ceramide (Molecular Probes, Inc., Eugene, Oreg.), which localizes to the Golgi complex. After ceramide staining, the cells were permeabilized with 2% paraformaldehyde–0.01 M PBS–0.05% Triton-X 100 for 1 h, washed five times in PBS, and blocked with 5% normal goat serum in PBS for 1 h. The primary VZV-specific antibody, diluted with 1% normal goat serum, was added for 1 h at 37°C; primary antibodies 6B5, specific for gI, and 3G8, specific for gE, were used at dilutions of 1:500 and 1:450, respectively (6B5 was kindly provided by Charles Grose; 3G8 was kindly provided by Bagher Forghani, California Department of Health Services, Berkeley). The secondary goat anti-mouse immunoglobulin G antibody, conjugated with fluorescein isothiocyanate or Texas red (Molecular Probes), was added to the wells for 30 min at 37°C. After washing, the slides were mounted with Vectashield (Vector Laboratories, Inc., Burlingame, Calif.) and examined with a Molecular Dynamics MultiProbe 2010 laser scanning confocal microscope (Fig. 5A to I) or an Applied Precision DeltaVision deconvolution microscope (Fig. 5J to L). The data were transferred to graphics software (Adobe Photoshop version 3.0) and printed with a Tektronix Phaser 440 dye sublimation printer.

RESULTS

Failure to generate infectious VZV from cosmids with a dual deletion of gE and gI. Based on observations that the gE and gI proteins of HSV-1, BHV, PRV, and equine herpesvirus are dispensable for the replication of these alphaherpesviruses in tissue culture (23, 32, 37, 38, 52, 53), initial experiments were done to determine whether both gE and gI could be deleted from VZV without blocking viral replication in melanoma cells. The removal of VZV nucleotides 114414 to 117355 from pVSpe21ΔAvrII resulted in a complete deletion of ORF67 along with 83 bp 3′ of the ORF67 start site (Fig. 1, line 4). This deletion also included the 250-bp region between ORF67 and ORF68 as well as the 1,547 bp extracellular domain of ORF68. The 321-bp C-terminal sequences that encode the transmembrane and intracellular domains of gE were intact but were not expected to be transcribed since the putative promoter of ORF68 was removed.

Cotransfection of the overlapping segments of VZV DNA from cosmids pVFsp4, pVSpe5, pVPme19, and the intact pVSpe21 consistently yielded infectious VZV isolates, designated rOka, with plaques visible within 5 to 6 days in melanoma cells. By 8 days after transfection, there were up to 140 plaques per 75-cm^2 flask. In contrast, no cytopathic changes were observed when four transfections were done in quadruplicate with pVSpe21ΔgI/gE and the other three cosmids. Varying the concentrations of pVSpe21ΔgI/gE from 2.0 to 3.0 μg/25-cm^2 flask and blind passage of transfected melanoma cells from all four experiments did not yield infectious virus. To exclude the possibility that an inhibitory substance that prevented VZV plaque formation was present in the pVSpe21ΔgI/gE preparation, transfections were carried out with a mixture of the intact pVSpe21 and the mutant cosmid. Typical cytopathic effects were observed, whereas infectious virus was not recovered in parallel experiments done with the mutant cosmid, despite blind passage. VZV proteins were not detected in extracts of cells recovered 13 days after transfection with the mutant cosmid and tested by a Western blot analysis with a high-titer polyclonal serum (data not shown).

Repeated efforts to derive a complementary cell line expressing gE for use in transfections with pVSpe21ΔgI/gE were unsuccessful, as has been reported previously, and may indicate that constitutive expression of VZV gE is toxic in mammalian cells (36).

Generation and replication characteristics of rOkaΔgI, a VZV mutant with a complete deletion of gI. A complete deletion of ORF67 was made to ensure that the altered phenotype observed in melanoma cells infected with OkaΔgI-N was due to a loss of gI function and not to the possible synthesis of a partial gene product containing the C-terminal region of gI. To delete the full ORF67 sequence, a restriction site was introduced between ORF67 and ORF68 by PCR. We deleted VZV nucleotides 114414 to 115563, which included the entire ORF67 gene, along with 83 bp 3′ of ORF67 and 5 bp 5′ of ORF67 (Fig. 1).

Infectious virus was recovered after transfection of pVSpe21ΔgI along with the three intact cosmids in seven experiments done in quadruplicate. The pattern of initial plaque formation and morphology was similar to that for rOkaΔgI-N and took 5 days longer than transfections done with intact

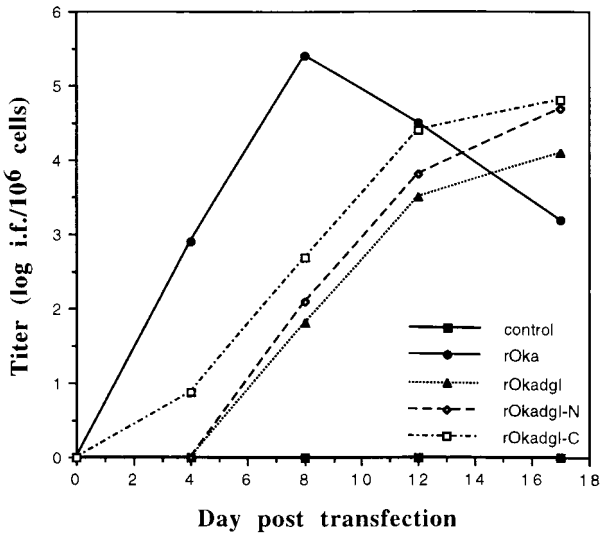

FIG. 2. Initial replication kinetics of gI deletion mutants and rOka derived from cosmid transfection into melanoma cells. Virus titer was determined at days 4, 8, 12, and 17 after transfection of the VZV cosmids into melanoma cells. After 5 to 6 days, the number of plaques was counted in triplicate wells. The average number of plaques was divided by the number of cells in the inoculum to calculate infectious foci (i.f.) per cell.

pVSpe21. rOkaΔgI reached peak titer at 17 days after transfection, compared to 8 days for rOka (Fig. 2). After the mutant virus was passaged several times in melanoma cells, the maximum titer of infectious virus was recovered from cells infected with rOkaΔgI at 3 days after infection, compared with 2 days for rOka (data not shown). Despite passage, the maximum titer of rOkaΔgI was 2.1 ± 0.05 SE (standard error) infectious foci/10^3cells, compared to 2.9 ± 0.01 SE infectious foci/10^3cells for rOka ($P = 0.0034$) (data not shown). The plaque size was distinctly smaller than for the parental virus (Fig. 3). The mean size of plaques produced by rOkaΔgI was 0.40 mm ± 0.14 SD (standard deviation), which was significantly smaller than for rOka ($P = 0.0001$). Differences from rOka growth and plaque phenotype were equivalent whether 60% of the N terminus of gI or all of gI was deleted.

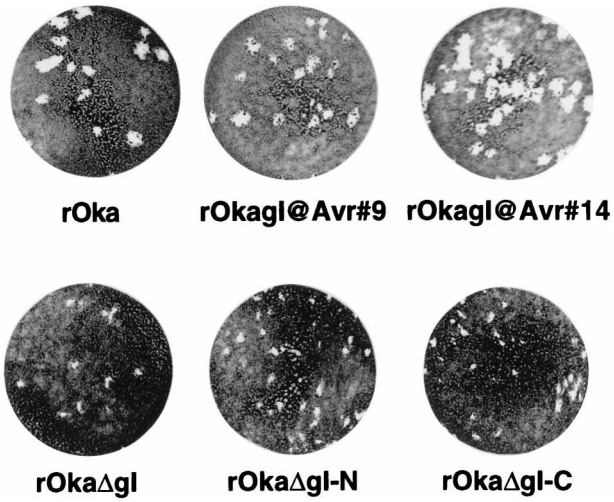

FIG. 3. Altered plaque formation in melanoma cells infected with gI deletion mutants. Melanoma cells infected with rOka, rOkagI@Avr#9, rOkagI @Avr#14, rOkaΔgI, rOkaΔgI-N, or rOkaΔgI-C) were fixed and stained with crystal violet 5 to 6 days after inoculation. Individual plaques were measured to calculate the mean plaque size produced by each virus.

Two separate clones of rOkaΔgI were characterized by Southern blot analysis, confirming the loss of a *Kpn*I restriction site that yielded a single fragment of 6.3 kb in rOkaΔgI (data not shown). By PCR, a decrease in DNA fragment size from 3.8 kb for rOka to 2.6 kb for rOkaΔgI was shown in assays using cosmid or viral DNA as the template, and sequence analysis of the PCR products demonstrated the expected changes (data not shown).

Generation and replication characteristics of rOkaΔgI-N, a VZV deletion mutant lacking the N-terminal region of gI. Initial plaque formation required 5 days longer than the control transfections done with intact pVSpe21 (Fig. 2). rOkaΔgI-N did not reach peak titer until 17 days after transfection, compared to 8 days for the parental strain, rOka (Fig. 2). After the mutant virus was passaged several times in melanoma cells, rOkaΔgI-N had a peak titer at 3 days postinfection, compared with 2 days for rOka (data not shown). rOkaΔgI-N also had a peak titer of 2.3 ± 0.1 SE infectious foci/10^3cells, compared to 2.9 ± 0.01 SE infectious foci/10^3cells ($P = 0.03$) for rOka (data not shown). In addition, the plaque size for rOkaΔgI-N was distinctly smaller than for the parental virus (Fig. 3). The mean size of plaques produced by infection of melanoma cells with rOka was 0.89 mm ± 0.28 SD, compared to 0.44 mm ± 0.13 SD for rOkaΔgI-N ($P = 0.0001$).

Use two separate clones of rOkaΔgI-N, Southern blot analysis of VZV DNA, PCR amplification across the mutated region, and sequencing of the PCR products from the mutated cosmid DNA yielded the expected changes (data not shown).

Generation and replication characteristics of rOkaΔgI-C, a VZV mutant lacking the C terminus of gI. A peptide sequence of gI that binds to gE has been identified in the N-terminal region of gI (34). To determine whether the presence of the N terminus of gI was sufficient to restore the replication and plaque size characteristics of rOka, a C-terminal deletion mutant was made. The mutant rOkaΔgI-C contains a deletion of nucleotides 115124 to 115563 from VZV DNA, of which the remaining nucleotides, 114414 to 115124, encode most of the extracellular domain and the N-terminal sequence of gI, including the sequence encoding the gE-binding peptide. In spite of the presence of this domain, the phenotype of rOkaΔgI-C resembled those of the rOkaΔgI and rOkaΔgI-N mutants.

Infectious virus was recovered after transfection of pVSpe21ΔgI-C with the intact cosmids. The initial plaque phenotype and the interval to plaque formation were similar to those for rOkaΔgI-N and rOkaΔgI, plaque formation requiring 5 days longer than in control transfections done with intact pVSpe21 in parallel. The peak titer of rOkaΔgI-C occurred at 17 days after transfection, compared to 8 days for rOka (Fig. 2). Maximum growth of rOkaΔgI-C after passage was detected at 2 days, which was the same as for rOka and 1 day earlier than for rOkaΔgI or rOkaΔgI-N (data not shown). The peak titer of rOkaΔgI-C was 2.4 ± 0.01 SE infectious foci/10^3cells, which was the same as for rOkaΔgI-N ($P = 0.42$), slightly higher than for rOkaΔgI ($P = 0.02$), and lower than for rOka ($P = 0.0001$) (data not shown). The mean size of plaques produced by rOkaΔgI-C was 0.35 mm ± 0.10 SD, which was significantly smaller than for rOka ($P = 0.0001$) (Fig. 3). The complete deletion of gI resulted in the most delayed growth rate and the least production of infectious virus, while preservation of the N terminus was associated with slightly better replication. However, all of the gI deletion mutants had significant reductions in infectivity and smaller plaque size in melanoma cells compared to rOka.

Two separate clones of rOkaΔgI-C were made to confirm

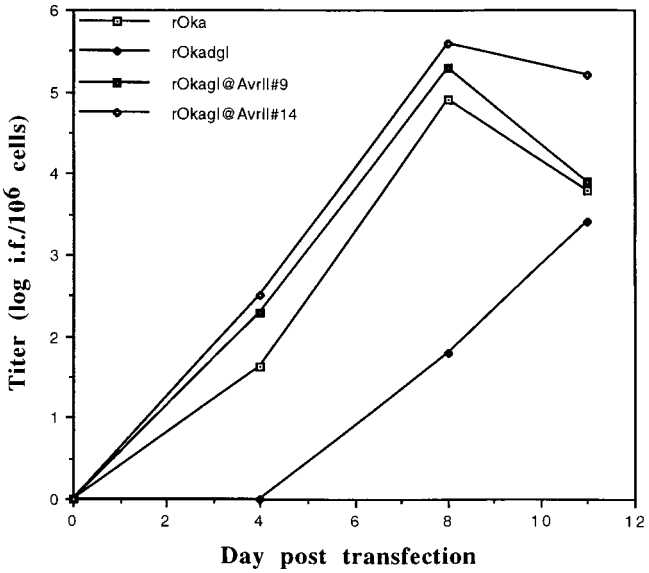

FIG. 4. Initial replication kinetics of gI deletion mutants with restored expression of gI. Infectious virus titers were determined at days 4, 8, and 11 after transfection of the VZV cosmids into melanoma cells. After 5 days, the number of plaques was counted in triplicate wells. The average number of plaques was divided by the number of cells in the inoculum to calculate the number of infectious foci (i.f.) per cell.

the association of the altered phenotype with the expected deletions in gI. A reduction in DNA fragment size from 3.8 kb in rOka to 3.3 kb in rOkaΔgI-C was demonstrated and sequencing the PCR products from cosmid and viral DNA had the expected deletion of the C terminus (data not shown).

Generation and replication characteristics of rOkagI@Avr with insertion of the gI gene into a novel *Avr*II site. To show that the altered replication characteristics of the gI deletion mutants were caused by the absence of the ORF67 gene product, ORF67, including regions spanning the upstream and downstream regions, was inserted into the unique *Avr*II restriction site in the pVSpe21ΔgI cosmid. The ORF67 coding sequence was cloned into the cosmid vector in both orientations, and the cosmids were designated pVSpe21gI@Avr#9 and pVSpe21gI@Avr#14 (Fig. 1).

Infectious virus was recovered by transfection of pVSpe21gI@Avr#9 or pVSpe21gI@Avr#14 with the other three cosmids, regardless of the orientation of gI. The initial plaque morphology and replication kinetics were indistinguishable from those of rOka, with plaques forming at 5 days post-transfection. The resulting viruses, designated rOka-gI@Avr#9 and rOka-gI@Avr#14, had peak titers at day 8 after transfection, 5.3 ± 0.1 and 5.6 ± 0.0 SE infectious foci/10^6cells, that were equal to that for rOka, 4.9 ± 0.25 SE infectious foci/10^6cells (Fig. 4). In contrast, rOkaΔgI showed a gradual increase for 11 days after transfection and failed to reach an equivalent peak titer. The mean size of plaque sizes produced rOkagI@Avr#9 was 0.68 mm ± 0.24 SD, which was somewhat smaller than for rOka (0.89 mm ± 0.28 SD) ($P = 0.003$); the plaque size of rOkagI@Avr#14 was 0.70 mm ± 0.16 SD ($P = 0.003$ compared to rOka) (Fig. 3). As for rOka, the plaque size observed with both of the gI-repaired viruses was increased markedly compared to that observed with rOkagIΔgI ($P = 0.0001$ and $P = 0.0001$, respectively).

The presence of the expected deletion in the original ORF67 site and the addition of ORF67 into the unique *Avr*II site were confirmed by PCR. The original deletion of ORF67 was associated with a decrease in DNA fragment size from 3.8 kb in rOka to 2.6 kb in rOka-gI@Avr#9 and rOka-gI@Avr#14 (data not shown). PCR amplification across the unique *Avr*II site demonstrated an increase in fragment size from 1.1 kb in rOka to 2.5 kb in rOkagI@Avr#9 and rOkagI@Avr#14 resulting from the insertion of ORF67 (data not shown). The PCR products of the respective cosmid and viral DNAs were sequenced to verify the gI deletion and insertion mutations (data not shown).

Disruption of syncytium formation by deletion of gI. Melanoma cells infected with rOka or the mutants rOkaΔgI, rOkaΔgI-N, rOkaΔgI-C, rOka-gI@Avr#9, and rOka-gI@Avr#14 were examined by confocal microscopy to further analyze the effects of gI deletion (Fig. 5). Syncytium characteristic of VZV infection, with extensive formation of polykaryocytes, were observed in cells infected with rOka or with the mutant strains in which gI expression was restored. In these multinucleated cells, the nuclei were organized in a regular pattern encircling centralized Golgi bodies which were demonstrated by staining with TR ceramide, a marker for Golgi localization (Fig. 5B and C). Recombinant strains in which gI production was intact also induced the formation of viral "highways" between cells (Fig. 5D and E) (28). In contrast, infection with all of the gI deletion mutants demonstrated disrupted syncytia. Cells had multiple nuclei, but their arrangement was disorganized and viral highways were not detected (Fig. 5G to I).

Analysis of the effects of gI deletion on gE trafficking and maturation. Because of the change in growth characteristics of the gI deletion mutants, we used confocal microscopy to examine the effects of removing gI on the maturation and cellular location of gE (Fig. 5). Melanoma cells infected with rOka virus or the mutants rOkaΔgI, rOkaΔgI-N, rOkaΔgI-C, rOka-gI@Avr#9, and rOka-gI@Avr#14 were stained with the anti-gE monoclonal 3G8 and TR ceramide 32 h after transfection. At this early time point, the expression of gE was restricted to the Golgi complex in cells infected with rOka and all of the mutants (data not shown). By 56 h after infection, gE was present in a diffuse distribution in infected cell membranes when intact gI was present, as shown in cells infected with rOka, rOkagI@Avr#9, and rOkagI@Avr#14 (Fig. 5C, E, and F). In contrast, gE expression was altered significantly when cells were infected with each of the gI deletion mutants (Fig. 5G to I). The gE trafficked to the cell surface, but its distribution in the absence of gI was in a localized, punctate pattern. No synthesis of gI was detected in cells infected with rOkaΔgI (data not shown) or rOkaΔgI-N (Fig. 5J), but specific binding of the anti-gI monoclonal 6B5 was observed after infection with rOkaΔgI-C (Fig. 5K). Nevertheless, the abnormal pattern of gE localization persisted despite the expression of the truncated form of gI, which contained a peptide sequence in the extracellular domain that is known to bind gE (34). The expression of gI was diffuse in cells infected with rOka, whereas the truncated form of gI was detected in the same localized, punctate pattern as observed for gE (Fig. 5K and L).

Initial experiments using fluorescence-activated cell sorting analysis and immunohistochemistry to examine infected cells labeled with a monoclonal antibody to gE, B5, showed specific binding to gE made by rOka but no staining of gE in cells infected with the gI deletion mutants (data not shown). However, gE was detectable in cells infected with the gI deletion mutants when a different monoclonal antibody, 3G8, was used. These experiments suggested a change in gE conformation causing a loss of the B5 binding epitope. Further evidence of changes in the characteristics of gE made in cells infected with the gI deletion mutants was observed by Western blot analysis

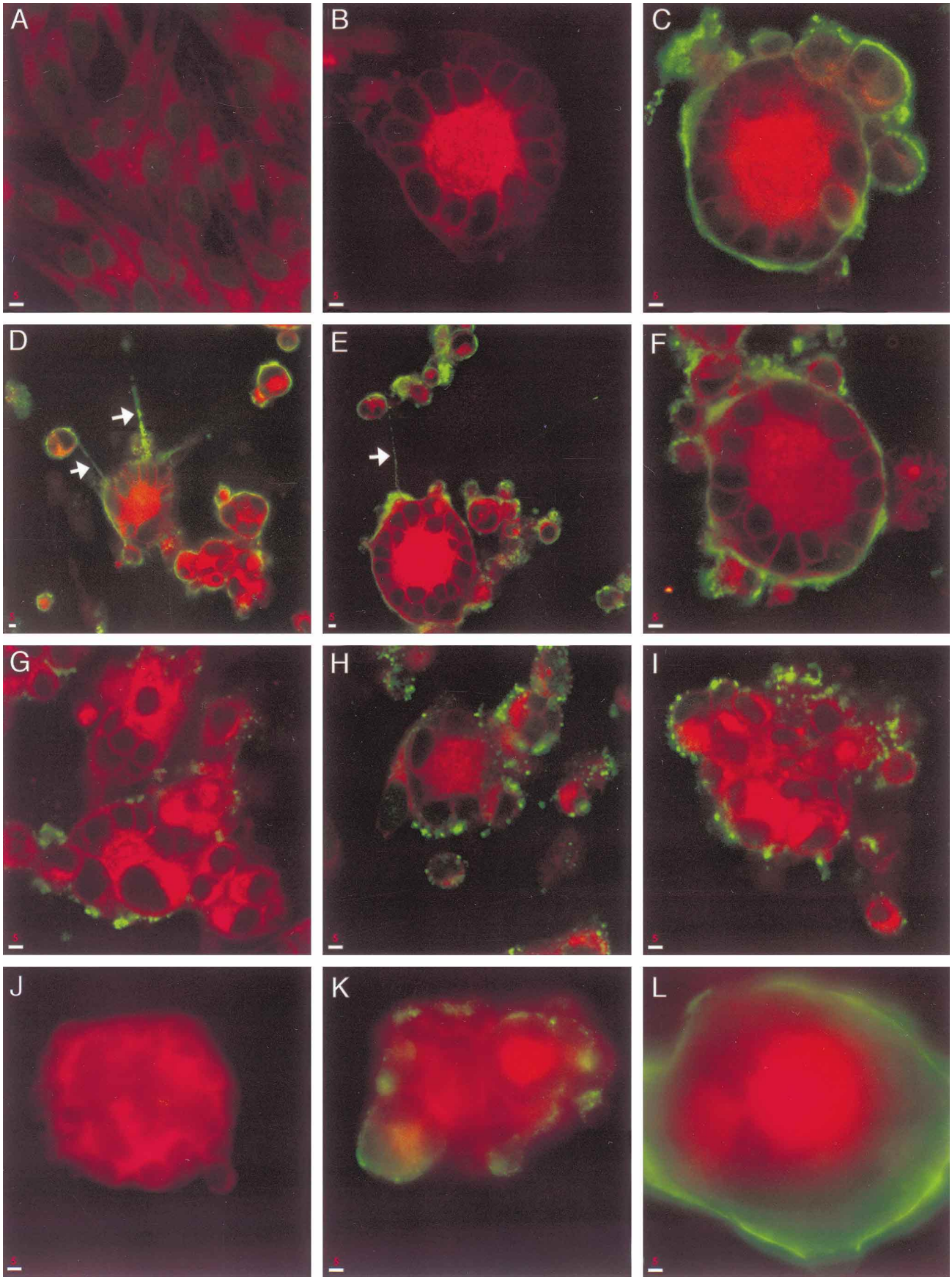
A
B
C
D
E
F
G
H
I
J
K
L

FIG. 5. Altered syncytium formation and cell surface localization of gE and gI cells infected with gI deletion mutants. Confocal microscopy was performed on permeabilized melanoma cells infected with rOka, gI deletion mutants, and mutants with restored gI expression. All cells were incubated with Golgi-specific BODIPY TR ceramide (red) and labeled with monoclonal antibody 3G8 (green) against gE (A and C to I) or monoclonal antibody 6B5 (green) against gI (J to L). Panel A shows uninfected melanoma cells, and panel B shows rOka-infected melanoma cells with fluorescein isothiocyanate-labeled secondary antibody and no primary antibody as a negative control; nuclei surrounding a centralized Golgi complex in a circular shape can be seen. Melanoma cells infected with rOka (C) or the gI-repaired virus rOkagI@Avr#14 (F) show diffuse staining with gE monoclonal antibody on the surface of the infected polykaryocyte. Viral highways, designated by arrows, are evident in cells infected with rOka (D) or the gI-repaired virus rOkagI@Avr#9 (E). The gI deletion mutants show a localized punctate staining of gE on the surface of cells infected with rOkaΔgI (G), rOkaΔgI-C (H), and rOkaΔgI-N (I) and a disorganized pattern of nuclei within polykaryocytes. gI is not detected in cells infected with rOkaΔgI-N (J) but is present in a localized distribution on the surface of rOkaΔgI-C infected cells (K). gI expression is diffuse on the surface of rOka-infected cells (L). Cells were examined with a Molecular Dynamics MultiProbe 2010 laser scanning confocal microscope (A to I) or an Applied Precision Delta Vision deconvolution microscope (J to L).

(Fig. 6). The mature form of gE, 98 kDa, was found in cells infected with rOka or with the gI mutants and stained with the polyclonal rabbit antiserum directed against gE. The underglycosylated 73-kDa form was detected in cells infected with rOka and the repaired mutants (Fig. 6A, lanes 2 to 4) but was not detected in the cells infected with gI mutant viruses in assays using this antibody (Fig. 6A, lanes 5 and 6). However, the underglycosylated form was detected in cells infected with gI mutant viruses when monoclonal antibody 3B3, which is also specific for gE, was used (Fig. 6B). These differences in antibody binding patterns suggested a change in conformation of the immature form of gE, with a loss of the polyclonal rabbit antiserum binding epitopes. Figure 6B also indicates that the level of gE expression is consistent among the various VZV strains tested.

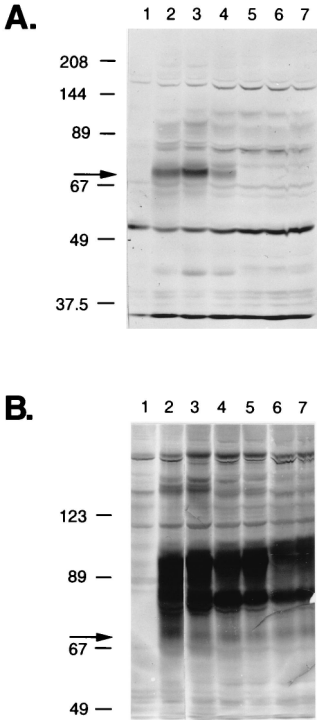

FIG. 6. Western blot analysis of gE expression in gI deletion mutants. Infected cell lysates were boiled in sample buffer, run on a 10% polyacrylamide gel, and transferred to a nitrocellulose membrane. Polyclonal rabbit antiserum anti-Vac-gE (A) or monoclonal antibody 3B3 (B) against gE were used as probes and detected with a biotinylated secondary antibody labeled with horseradish peroxidase. (A) Underglycosylated forms of gE (arrow) are detected at 73 kDa in the extracts from cells infected with rOka (lane 2) and gI deletion mutants with gI expression restored, rOkagI@Avr#9 (lane 3) and rOkagI@Avr#14 (lane 4). The 73-kDa form is not detected in uninfected melanoma cells (lane 1) or cells infected with gI deletion mutants rOkaΔgI-N (lane 5), rOkaΔgI (lane 6), and rOkaΔgI-C (lane 7). (B) Underglycosylated forms are detected with monoclonal antibody to gE in cells infected with rOka (lane 2), rOkagI@Avr#9 (lane 3), rOkagI@Avr#14 (lane 4), rOkaΔgI-C (lane 5), rOkaΔgI (lane 6), and rOkaΔgI-N (lane 7). Underglycosylated forms were not detected in uninfected melanoma cells (lane 1).

DISCUSSION

Our experiments using VZV cosmids demonstrated that gI was dispensable whereas gE appeared to be necessary for viral replication. Although infectivity was preserved, the deletion or mutation of gI inhibited the formation of syncytia which is a hallmark of VZV infection in tissue culture cells. VZV recombinants with complete or partial deletions of gI also consistently exhibited delayed replication kinetics and lower yields of infectious virus. The characteristic plaque morphology and replication pattern were restored by the insertion of the gI gene, ORF67, into a nonnative site, indicating that the changes were due to gI mutations rather than to disruption of promoter sequences or other regulatory regions affecting adjacent genes in the U_S segment or to random mutations elsewhere in the genome. The recovery of infectivity that occurred when ORF67 was cloned into the unique *Avr*II site between ORF65 and ORF66 also demonstrated that this site can be used to confirm the specificity of effects associated with other VZV genetic mutations and to evaluate the potential of VZV as a vector for the expression of foreign DNA sequences.

The consequences of VZV gI deletion or mutation on viral replication were similar to those described after disruptions of homologous genes in other alphaherpesviruses (7, 23, 37, 38, 52, 53). The plaque size of HSV-1 mutants that lacked gI expression was significantly smaller in fibroblasts or epithelial cells, whereas plaque size was almost equivalent to that of the parent strain in Vero cells, suggesting that gI is important for efficient cell-to-cell spread of HSV-1 in cell types that form tight junctions in vitro (17). The small plaque phenotype of the VZV gI deletion mutants provided further evidence that gI gene products contribute to fusion between cells infected with alphaherpesviruses and adjacent, uninfected cells. In the case of VZV, interference with mechanisms of cell-to-cell spread can also be expected to have the direct effect on infectious virus production that we observed because VZV is not released from infected cells in vitro.

The abnormal membrane fusion that occurred in cells infected with the VZV gI mutants could reflect loss of a function that is mediated by gI only, by gE-gI complexes, or by gE only. Like the homologous proteins of HSV-1 and other herpesviruses, VZV gI and gE oligomerize to form a noncovalently linked complex in infected or transfected cells (55). Using a baculovirus system, Kimura et al. showed that the gI and gE subunits were present in a 1:1 ratio and that the mature amino terminus of gI was required for heterodimer formation (34). If enhancement of fusion involves the presence of gE-gI complexes in the cell membrane, this function would have been eliminated in cells infected with rOkaΔgI and rOkaΔgI-N. By this hypothesis, the failure to restore normal VZV plaque

morphology by expression of the N terminus of gI in rOkaΔgI-C suggests that other regions of gI are also required for gE-gI binding. Alternatively, since oligomerization is concentration dependent, this change could reflect decreased heterodimer formation resulting from reduced synthesis of truncated gI (19). Conformational changes in truncated gI may also have prevented its proper interaction with gE even if sufficient concentrations of gI were made, because correct folding of the protein components must precede oligomerization in order for the subunits to associate. It is important to emphasize that taken together, the titer and plaque size experiments (Fig. 2 and 3) indicate that the absence of intact gI leads to a delay in growth kinetics which also manifests itself in a plaque morphology that remains restricted in size over time compared to wild-type VZV or the revertant VZV.

The disruption of syncytia in cells infected with rOkaΔgI, rOkaΔgI-N, and rOkaΔgI-C is consistent with the possibility that gE alone, rather than the presence of gE-gI complexes at the cell surface, facilitates membrane fusion and cell-to-cell spread of VZV. In this case, the effects that we observed may be due to changes in gE conformation and trafficking that occur in the absence of a gI chaperone function. A requirement for gI to achieve maturation or transport of gE has been observed in other alphaherpesviruses. For example, only immature forms of gE were made by feline herpesvirus and BHV mutants that lacked gI (41, 53). In feline herpesvirus, gE was retained in the ER without gE-gI complex formation, and gI was required for efficient movement of gE to the cell surface in PRV-infected cells (41, 52). The trafficking of VZV gE to the cell membrane was expected despite deletion of gI from the virus because surface localization has been observed after expression of gE from plasmid constructs (36, 55, 56). Zhu et al. showed that VZV gE has a targeting sequence for the trans-Golgi network which was sufficient for independent transport of the protein (57). Although we have no evidence of a direct role for gE in mediating membrane fusion, our experiments demonstrate that gE plays an important role in virus spread, as has been shown for other herpesvirus gE proteins. Our suggestion that gE contributes to membrane fusion is based on the fact that VZV is a highly cell associated virus and syncytium formation, caused by fusion of infected cell membranes with neighboring cells, is particularly prominent in the cell-to-cell spread of this virus. VZV is probably more dependent on this mechanism of cell-to-cell spread than HSV, which in contrast releases virus into the intercellular spaces and infects adjacent cells.

In our experiments, VZV gE was not retained in the ER or Golgi complex in cells infected with rOkaΔgI, rOkaΔgI-N, or rOkaΔgI-C, but confocal microscopy revealed that cell surface expression of gE was changed to a clumped, punctate pattern which differed dramatically from the diffuse distribution of gE seen in cells infected with intact rOka or the gI-repaired recombinants. The synthesis of VZV gE in rOkaΔgI, or when only truncated gI was made in rOkaΔgI-C, was associated with a conformational change in the underglycosylated form, as shown by the loss of an antibody-binding epitope. These results indicated that some posttranslational modifications of gE required the presence of intact gI within virus-infected cells. Transfection experiments have shown that although VZV gE can be processed in the ER and Golgi complex when expressed independently of gI, the forms of gE differ from those detected when gE was coexpressed with gI (54, 55). Alterations in VZV gE folding when it is made in the absence of gI may diminish its capacity to enhance membrane fusion at the cell surface during virus replication. The patched localization of gE on the membrane of cells infected with the gI deletion mutants further suggested that the process of gE endocytosis and recycling may be disrupted in the absence of gI (45). Under normal conditions, the VZV glycoprotein gH requires complexing with gL for transport to the cell surface. However, gE has been reported to compensate for the absence of the gL chaperone, with gH being detected on the cell surface in a patched pattern (21). Confocal experiments were performed with cells infected with the gI deletion mutants to determine whether gE might interact with gH in the absence of gI, but no colocalization of gE with gH was detected (data not shown).

In addition to incorporating into gE-gI heterodimers, the underglycosylated form of VZV gE forms dimers of 130 kDa that appear diffusely on the surfaces of infected or transfected cells (46). Olson et al. have suggested that dimerization may occur in the ER soon after gE synthesis or within the cell membrane after underglycosylated forms of gE are chaperoned by gI to the surface and that dimerization may be a necessary condition for a cell surface receptor function (46). The change that we observed in the conformation of the underglycosylated, monomeric form of gE made by rOkaΔgI, rOkaΔgI-N, and rOkaΔgI-C may have interfered with its dimerization. If enhanced fusion is mediated by gE dimers, the absence of intact gI could decrease syncytium formation indirectly by effects on gE dimerization. The mature form of VZV gE is a phosphorylated protein, modified posttranslationally by serine/threonine casein kinase II (46). Phosphorylation may play a role in the intracellular sorting of glycoproteins as they exit the trans-Golgi. In transfection experiments, C-terminal deletions of gI markedly reduced phosphorylation, and phosphorylation-deficient gE was processed faster than wild-type gE (46, 54, 56). It has been suggested that the phosphorylation and dephosphorylation of gE in HSV-1 as well as VZV affect trafficking events involved in cell-to-cell spread and viral egress (17, 28). An effect on phosphorylation could explain the fact that deletion of the C-terminal sequences of gI was associated with an altered pattern of VZV replication in tissue culture cells, despite preservation of the gE-gI binding site in the N-terminal segment. VZV gE may require intact gI to act as a cofactor for phosphorylation as well as to facilitate the correct folding of gE.

The failure of the VZV gI deletion mutants to form normal polykaryocytes or to create the viral highways that extend from cells infected with wild-type VZV, as described by Harson and Grose (28), was evident by confocal microscopy. Deletion or truncation of gI changed how VZV replication within the cell remodels cellular membranes to enhance transmission. Nevertheless, some cell fusion leading to polykaryocyte formation occurred despite gI mutation. Herpesviruses appear to have an inherent redundancy in proteins that can mediate this essential function or in proteins that can participate in the required complexes. The persistence of membrane fusion in cells infected with gI deletion mutants was probably mediated by VZV gH, which continued to traffic to the cell surface. The gH-gL complex has been shown to mediate extensive cell membrane fusion in transfection experiments when no other VZV glycoproteins were expressed (21). Duus and Grose found that gE facilitated the cell surface expression of gH in the absence of its usual partner, gL, but the gE-gH interaction led to a distinctive patching of protein expression (21). We considered that gH might have substituted for gI in gE binding and transport in the gI mutants, particularly because of the punctate pattern of gE staining, but colocalization of gE and gH was not detected. In addition to diminished syncytium formation, the polykaryocytes generated without intact gI exhibited a very disorganized arrangement of nuclei. The appearance of these multinucleated cells contrasted markedly with the symmetric

band of nuclei encircling a centralized Golgi complex that was observed in cells infected with intact or gI-repaired VZV recombinants. How gI or the gE-gI complex is involved in creating this intracellular event, as well as how it contributes to efficient replication of the virus, warrants further investigation. Experiments are also in progress to address whether the truncated gI, expressed in rOkaΔgI-C, can interact directly with gE and the effect of gI deletion on the phosphorylation pattern of gE.

Since gI was dispensable for infectivity, the consistent failure to generate mutant virus from cosmids when the ORF68 was also removed suggested that gE was necessary for VZV replication. The gE homolog is dispensable for replication of other alphaherpesviruses in tissue culture (7, 23, 32, 37, 38, 52, 53). However, VZV gE is the most abundant glycoprotein in the virion envelope and in infected cells (14, 25). Recent observations demonstrate that gE has targeting sequences for the trans-Golgi network within the cytoplasmic domain which may have a critical role in the virion envelopment process (1, 57). Since VZV is the only alphaherpesvirus that lacks a gene encoding gD in the U_S region, VZV gE may mediate necessary functions that are usually associated with gD, which is indispensable in most alphaherpesviruses. Amino acid sequence comparisons have suggested a distant relationship between gE and gD and other glycoproteins in the U_S region, implying that duplication and divergence of glycoprotein genes in the U_S may have occurred during the evolution of the alphaherpesviruses (39). gD may have acquired functions that are carried out by gE in VZV. The possibility that gE and gD have duplicated functions is supported by the observation that the loss of gD from PRV was compensated for by repeated passage of a gD deletion mutant and that Marek's disease virus replicates in tissue culture even though its gD homolog is not expressed (47, 49).

The newly licensed varicella vaccine is derived from the Oka strain, from which the VZV cosmids used in our experiments were generated. Although clinical studies document its safety and efficacy as a live attenuated vaccine, the Oka strain retains the capacity to establish latency and to reactivate from dorsal root ganglia (3). In vivo, intact gI expression was required for the efficient spread of HSV-1 between neurons and for the neurotropism of PRV (17, 22). The deletion of the gI homolog, designated gp63, from PRV, as well as the gE homolog, interfered with its infectivity for specific classes of neurons in the rat retina (8, 52). An evaluation of the effect of VZV gI deletion on neurovirulence, using the rat model of VZV neurotropism, is in progress (16). If VZV gI contributes to infection of dorsal root ganglion cells, the vaccine strain might be further attenuated for neurovirulence by deleting gI.

ACKNOWLEDGMENTS

This work was supported by Public Health Service grants AI20459, AI36884, and CA49605 and fellowship 5 F31 GM14843-05.

We thank Linda Lew for technical assistance and George Kemble for providing the VZV cosmids and advice about their use. We thank Charles Grose, Bagher Forghani, and Paul Kinchington for providing antibody reagents. We thank Susan Palmieri and Chris Canfield, Stanford University Cell Sciences Imaging Facility, for help with the confocal microscopy.

REFERENCES

1. **Alaconda, A., U. Bauer, and B. Hoflack.** 1996. A tyrosine-based motif and a casein kinase II phosphorylation site regulate the intracellular trafficking of the varicella-zoster virus glycoprotein I, a protein localized in the trans-Golgi network. EMBO J. **5:**6096–6110.
2. **Arvin, A. M.** 1996. Varicella-zoster virus, p. 2547–2585. *In* B. N. Fields, D. M. Knipe, P. M. Howley, R. M. Chanock, J. L. Melnick, T. P. Monath, B. Roizman, and S. E. Straus (ed.), Fields virology. Lippincott-Raven Publishers, Philadelphia, Pa.
3. **Arvin, A. M., and A. A. Gershon.** 1996. Live attenuated varicella vaccine. Annu. Rev. Microbiol. **50:**59–100.
4. **Arvin, A. M., E. Kinney-Thomas, K. Shriver, C. Grose, C. M. Koropchak, E. Scranton, A. E. Wittek, and P. S. Diaz.** 1986. Immunity to varicella-zoster viral glycoproteins, gp I (gp 90/58) and gp III (gp 118), and to a nonglycosylated protein, p 170. J. Immunol. **137:**1346–1351.
5. **Arvin, A. M., S. M. Solem, C. M. Koropchak, T. E. Kinney, and S. G. Paryani.** 1987. Humoral and cellular immunity to varicella-zoster virus glycoprotein gpI and to a non-glycosylated protein, p170, in the strain 2 guinea-pig. J. Gen. Virol. **68:**2449–2454.
6. **Babic, N., B. Klupp, A. Brack, T. C. Mettenleiter, G. Ugolini, and A. Flamand.** 1996. Deletion of glycoprotein gE reduces the propagation of pseudorabies virus in the nervous system of mice after intranasal inoculation. Virology **219:**279–284.
7. **Balan, P., N. Davis-Poynter, S. Bell, H. Atkinson, H. Browne, and T. Minson.** 1994. An analysis of the in vitro and in vivo phenotypes of mutants of herpes simplex virus type 1 lacking glycoproteins gG, gE, gI or the putative gJ. J. Gen. Virol. **75:**1245–1258.
8. **Card, J. P., M. E. Whealy, A. K. Robbins, and L. W. Enquist.** 1992. Pseudorabies virus envelope glycoprotein gI influences both neurotropism and virulence during infection of the rat visual system. J. Virol. **66:**3032–3041.
9. **Cines, D. B., A. P. Lyss, M. Bina, R. Corkey, N. A. Kefalides, and H. M. Friedman.** 1982. Fc and C3 receptors induced by herpes simplex virus on cultured human endothelial cells. J. Clin. Invest. **69:**123–128.
10. **Cohen, J. I., and K. E. Seidel.** 1993. Generation of varicella-zoster virus (VZV) and viral mutants from cosmid DNAs: VZV thymidylate synthetase is not essential for viral replication in vitro. Proc. Natl. Acad. Sci. USA **90:**7376–7380.
11. **Cohen, J. I., and S. E. Straus.** 1996. Varicella-zoster virus and its replication, p. 2525–2545. *In* B. N. Fields, D. M. Knipe, P. M. Howley, R. M. Chanock, J. L. Melnick, T. P. Monath, and B. Roizman (ed.), Fields virology. Lippincott-Raven Publishers, Philadelphia, Pa.
12. **Costa, J., C. Yee, Y. Nakamura, and A. Rabson.** 1978. Characteristics of the Fc receptor induced by herpes simplex virus. Intervirology **10:**32–39.
13. **Davison, A. J., and J. E. Scott.** 1986. The complete DNA sequence of varicella-zoster virus. J. Gen. Virol. **67:**1759–1816.
14. **Davison, A. J., D. J. Waters, and C. M. Edson.** 1986. Identification of the products of a varicella-zoster virus glycoprotein gene. J. Gen. Virol. **66:**2237–2242.
15. **Davis-Poynter, N., S. Bell, T. Minson, and H. Browne.** 1994. Analysis of the contributions of herpes simplex virus type 1 membrane proteins to the induction of cell-cell fusion. J. Virol. **68:**7586–7590.
16. **Debrus, S., C. Sadzot-Delvaux, A. F. Nikkels, J. Piette, and B. Rentier.** 1995. Varicella-zoster virus gene 63 encodes an immediate-early protein that is abundantly expressed during latency. J. Virol. **69:**3240–3245.
17. **Dingwell, K. S., C. R. Brunetti, R. L. Hendricks, Q. Tang, M. Tang, A. J. Rainbow, and D. C. Johnson.** 1994. Herpes simplex virus glycoproteins E and I facilitate cell-to-cell spread in vivo and across junctions of cultured cells. J. Virol. **68:**834–845.
18. **Dingwell, K. S., L. C. Doering, and D. C. Johnson.** 1995. Glycoproteins E and I facilitate neuron-to-neuron spread of herpes simplex virus. J. Virol. **69:**7087–7098.
19. **Doms, R. W., R. A. Lamb, J. K. Rose, and A. Helenius.** 1993. Minireview: folding and assembly of viral membrane proteins. Virology **193:**545–562.
20. **Dubin, G., S. Basu, D. L. Mallory, M. Basu, R. Tal-Singer, and H. M. Friedman.** 1994. Characterization of domains of herpes simplex virus type 1 glycoprotein E involved in Fc binding activity for immunoglobulin G aggregates. J. Virol. **68:**2478–2485.
21. **Duus, K. M., and C. Grose.** 1996. Multiple regulatory effects of varicella-zoster virus (VZV) gL on trafficking patterns and fusogenic properties of VZV gH. J. Virol. **70:**8961–8971.
22. **Enquist, L. W.** 1994. Infection of the mammalian nervous system by pseudorabies virus (PRV). Semin. Virol. **5:**221–231.
23. **Flowers, C. C., and D. J. O'Callaghan.** 1992. The equine herpesvirus type 1 (EHV-1) homolog of herpes simplex virus type 1 US9 and the nature of a major deletion within the unique short segment of the EHV-1 KyA strain genome. Virology **190:**307–315.
24. **Forghani, B., K. W. Dupuis, and N. J. Schmidt.** 1990. Epitopes functional in neutralization of varicella-zoster virus. J. Clin. Microbiol. **28:**2500–2506.
25. **Grose, C.** 1980. The synthesis of glycoproteins in human melanoma cells infected with varicella-zoster virus. Virology **101:**1–9.
26. **Grose, C.** 1990. Glycoproteins encoded by varicella-zoster virus: biosynthesis, phosphorylation, and intracellular trafficking. Annu. Rev. Microbiol. **44:**59–80.
27. **Grose, C., and P. A. Brunell.** 1978. Varicella-zoster virus: isolation and propagation in human melanoma cells at 36 and 32°C. Infect. Immun. **19:**199–203.
28. **Harson, R., and C. Grose.** 1995. Egress of varicella-zoster virus from the melanoma cell: a tropism for the melanocyte. J. Virol. **69:**4994–5010.
29. **Haumont, M., A. Jacquet, M. Massaer, V. Deleersnyder, P. Mazzu, A. Bol-**

len, and P. Jacobs. 1996. Purification, characterization and immunogenicity of recombinant varicella-zoster virus glycoprotein gE secreted by Chinese hamster ovary cells. Virus. Res. **40:**199–204.
30. **Huang, Z., A. Vafai, J. Lee, R. Mahalingam, and A. R. Hayward.** 1992. Specific lysis of targets expressing varicella-zoster virus gpI or gpIV by $CD4^+$ human T-cell clones. J. Virol. **66:**2664–2669.
31. **Johnson, D. C., and V. Peenstra.** 1987. Identification of a novel herpes simplex virus type 1-induced glycoprotein which complexes with gE and binds immunoglobulin J. J. Virol. **61:**2208–2216.
32. **Kaashoek, M. J., A. Moerman, J. Madic, A. M. Rijsewijk, J. Quak, A. L. J. Gielkens, and J. T. Van Oirschot.** 1993. A conventionally attenuated glycoprotein E negative strain of bovine herpesvirus type 1 is an efficacious and safe vaccine. Vaccine **12:**439–444.
33. **Kemble, G.** Personal communication.
34. **Kimura, H., S. E. Straus, and R. K. Williams.** Varicella-zoster virus glycoproteins E and I expressed in insect cells form a hetero-dimer that requires the N-terminal domain of glycoprotein I. Virology, in press.
35. **Ligas, M., and D. Johnson.** 1988. A herpes simplex virus mutant in which glycoprotein D sequences are replaced by β-galactosidase sequences binds to but is unable to penetrate into cells. J. Virol. **62:**1486–1494.
36. **Litwin, V., W. Jackson, and C. Grose.** 1992. Receptor properties of two varicella-zoster virus glycoproteins, gpI and gpIV, homologous to herpes simplex virus gE and gI. J. Virol. **66:**3643–3651.
37. **Longnecker, R., S. Chatterjee, R. Whitley, and B. Roizman.** 1987. Identification of a herpes simplex virus 1 glycoprotein gene within a gene cluster dispensable for growth in cell culture. Proc. Natl. Acad. Sci. USA **84:**4303–4307.
38. **Longnecker, R., and B. Roizman.** 1986. Generation of an inverted herpes simplex virus 1 mutant lacking the L-S junction a sequences, an origin of DNA synthesis, and several genes including those specifying glycoprotein E and the alpha 47 gene. J. Virol. **58:**583–591.
39. **McGeoch, D. J.** 1990. Evolutionary relationships of virion glycoprotein genes in the S regions of alphaherpesvirus genomes. J. Gen. Virol. **71:**2361–2367.
40. **McTaggart, S. P., W. H. Burns, D. O. White, and D. C. Jackson.** 1978. Fc receptors induced by herpes simplex virus. Biol. Biochem. Prop. **121:**726–730.
41. **Mijnes, J. D. F., L. M. Van der Horst, E. Van Anken, M. C. Horzinek, P. J. M. Rottier, and R. J. De Groot.** 1996. Biosynthesis of glycoprotein E and I of feline herpesvirus: gE-gI interaction is required for intracellular transport. J. Virol. **70:**5466–5475.
42. **Moffat, J., M. D. Stein, H. Kaneshima, and A. M. Arvin.** 1995. Tropism of varicella-zoster virus for human $CD4^+$ and $CD8^+$ T lymphocytes and epidermal cells in SCID-hu mice. J. Virol. **69:**5236–5242.
43. **Montalvo, E. A., R. T. Parmley, and C. Grose.** 1985. Structural analysis of the varicella-zoster virus gp98-gp62 complex: posttranslational addition of N-linked and O-linked oligosaccharide moieties. J. Virol. **53:**761–770.
44. **Mulder, W., J. Pol, T. Kimman, G. Kok, J. Priem, and B. Peeters.** 1996. Glycoprotein D-negative pseudorabies virus can spread transneuronally via direct neuron-to-neuron transmission in its natural host, the pig, but not after additional inactivation of gE or gI. J. Virol. **70:**2191–2200.
45. **Olson, J., and C. Grose.** 1997. Endocytosis and recycling of varicella-zoster virus Fc receptor glycoprotein gE: internalization mediated by a YXXL motif in the cytoplasmic tail. J. Virol. **71:**4042–4054.
46. **Olson, J. K., G. A. Bishop, and C. Grose.** 1997. Varicella-zoster virus Fc receptor gE glycoprotein: serine/threonine and tyrosine phosphorylation of monomeric and dimeric forms. J. Virol. **71:**110–119.
47. **Parcells, M., A. Anderson, and R. Morgan.** 1994. Characterization of a Marek's disease virus mutant containing a lacZ insertion in the US6 (gD) homologue gene. Virus Genes **9:**5–13.
48. **Roizman, B., and A. E. Sears.** 1996. Herpes simplex viruses and their replication, p. 2231–2295. *In* B. N. Fields, D. M. Knipe, and P. M. Howley (ed.), Fields virology. Lippincott-Raven Publishers, Philadelphia, Pa.
49. **Schmidt, J., B. G. Klupp, A. Karger, and T. C. Mettenleiter.** 1997. Adaptability in herpesviruses: glycoprotein D-independent infectivity of pseudorabies virus. J. Virol. **71:**17–24.
50. **Vafai, A., and W. N. Yang.** 1991. Neutralizing antibodies induced by recombinant vaccinia virus expressing varicella-zoster virus gp IV. J. Virol. **65:**5593–5596.
51. **Van Zijl, M., W. Quint, J. Briaire, T. De Rover, A. Gielkens, and A. Berns.** 1988. Regeneration of herpesviruses from molecularly cloned subgenomic fragments. J. Virol. **62:**2191–2195.
52. **Whealy, M. E., J. P. Card, A. K. Robbins, J. R. Dubin, H. Rziha, and L. W. Enquist.** 1993. Specific pseudorabies virus infection of the rat visual system requires both gI and gp63 glycoproteins. J. Virol. **67:**3786–3797.
53. **Whitbeck, J. C., A. C. Knapp, L. W. Enquist, W. C. Lawrence, and L. J. Bello.** 1996. Synthesis, processing, and oligomerization of bovine herpesvirus 1 gE and gI membrane proteins. J. Virol. **70:**7878–7884.
54. **Yao, Z., and C. Grose.** 1994. Unusual phosphorylation sequence of gpIV (gI) component of the varicella-zoster virus gpI-gpIV glycoprotein complex (VZV gE-gI complex). J. Virol. **68:**4204–4211.
55. **Yao, Z., W. Jackson, B. Forghani, and C. Grose.** 1993. Varicella-zoster virus glycoprotein gpI/gpIV receptor: expression, complex formation, and antigenicity within the vaccinia virus-T7 RNA polymerase transfection system. J. Virol. **67:**305–314.
56. **Yao, Z., W. Jackson, and C. Grose.** 1993. Identification of the phosphorylation sequence in the cytoplasmic tail of the varicella-zoster virus Fc receptor glycoprotein gpI. J. Virol. **67:**4464–4473.
57. **Zhu, Z., Y. Hao, M. D. Gershon, R. T. Ambron, and A. Gershon.** 1996. Targeting of glycoprotein I (gE) of varicella-zoster virus to the trans-Golgi network by an AYRV sequence and an acidic amino acid-rich patch in the cytosolic domain of the molecule. J. Virol. **70:**6563–6575.
58. **Zuckerman, F., T. C. Mettenleiter, C. Schreurs, N. Sugg, and T. Ben-Porat.** 1988. Complex between glycoproteins gI and gp63 of pseudorabies virus: its effect on virus replication. J. Virol. **62:**4622–4626.